## ORIGINAL RESEARCH

Myeloid Deletion of Cdc42 Protects Liver From Hepatic Ischemia-Reperfusion Injury via Inhibiting Macrophage-Mediated Inflammation in Mice

Jing He,[1] Meng-Yu Tang,[2] Li-Xin Liu,[1,3] Chen-Xian Kong,[2] Wen Chen,[2] Lu Wang,[1] Shao-Bin Zhi,[1] Hong-Wei Sun,[1] Yu-Chun Huang,[1] Guo-Yu Chen,[4] Hong-Bo Xin,[1,2,3] and Ke-Yu Deng[1,2,3]

[1]The National Engineering Research Center for Bioengineering Drugs and Technology, Institution of Translation Medicine, Nanchang University, Nanchang, Jiangxi, PR China; [2]College of Life Science, Nanchang University, Nanchang, Jiangxi, PR China; [3]College of Pharmacy, Nanchang University, Nanchang, Jiangxi, PR China; and [4]The First Clinical Medical College, Nanchang University, Nanchang, Jiangxi, PR China
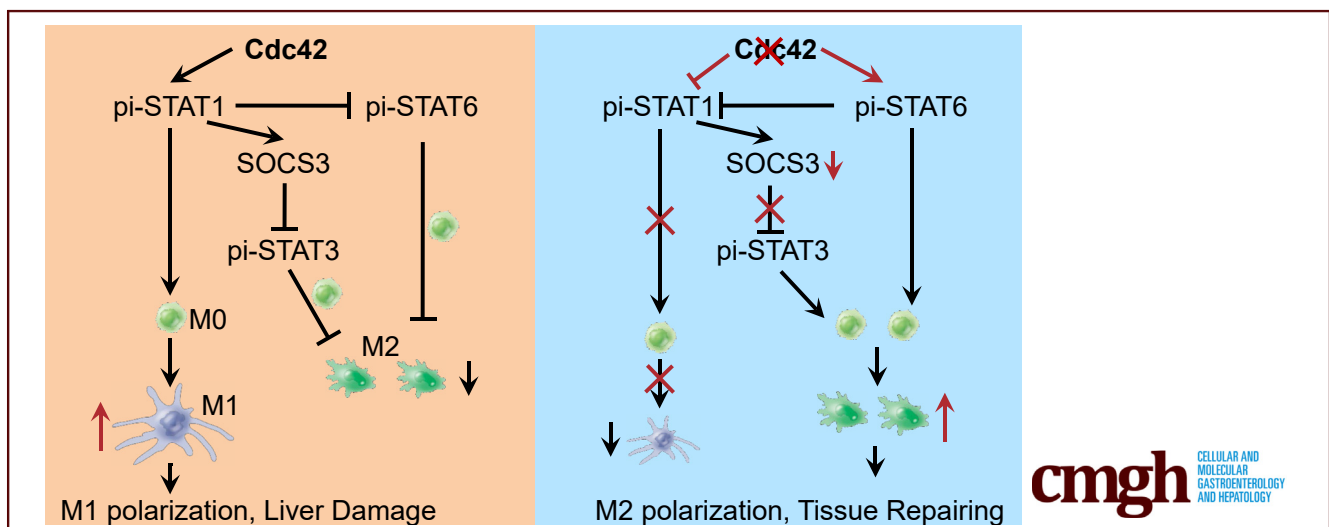
SUMMARY

Myeloid deletion of cell division cycle 42 (Cdc42) gene protected liver from hepatic ischemia reperfusion injury via suppressing infiltration of macrophages and proinflammatory response in mice. Inactivation or deficiency of Cdc42 reduced M1 polarization and enhanced M2-type polarization by suppressing STAT1-SOCS3 signaling and enhancing STAT3/STAT6 activation in macrophages.

BACKGROUND & AIMS: Hepatic ischemia-reperfusion injury (HIRI) often occurs in liver surgery, such as partial hepatectomy and liver transplantation, in which myeloid macrophage-mediated inflammation plays a critical role. Cell division cycle 42 (Cdc42) regulates cell migration, cytoskeleton rearrangement, and cell polarity. In this study, we explore the role of myeloid Cdc42 in HIRI.

METHODS: Mouse HIRI models were established with 1-hour ischemia followed by 12-hour reperfusion in myeloid Cdc42 knockout (Cdc42^{mye}) and Cdc42^{flox} mice. Myeloid-derived macrophages were traced with Rosa^{mTmG} fluorescent reporter under LyzCre-mediated excision. The experiments for serum or hepatic enzymic activities, histologic and immunologic analysis, gene expressions, flow cytometry analysis, and cytokine antibody array were performed.

RESULTS: Myeloid deletion of Cdc42 significantly alleviated hepatic damages with the reduction of hepatic necrosis and inflammation, and reserved hepatic functions following HIRI in mice. Myeloid Cdc42 deficiency suppressed the infiltration of myeloid macrophages, reduced the secretion of proinflammatory cytokines, restrained M1 polarization, and promoted M2 polarization of myeloid macrophages in livers. In addition, inactivation of Cdc42 promoted M2 polarization via suppressing the phosphorylation of STAT1 and promoting phosphorylation of STAT3 and STAT6 in myeloid macrophages. Furthermore, pretreatment with Cdc42 inhibitor, ML141, also protected mice from hepatic ischemia-reperfusion injury.

CONCLUSIONS: Inhibition or deletion of myeloid Cdc42 protects liver from HIRI via restraining the infiltration of myeloid macrophages, suppressing proinflammatory response, and promoting M2 polarization in macrophages. *(Cell Mol*

Hepatic ischemia-reperfusion injury (HIRI) inevitably occurs during partial hepatectomy and liver transplantation, which triggers the production of reactive oxygen species and hyperactive inflammation and leads to cellular damages and organ dysfunction.[1] Multiple cells including hepatocytes, Kupffer cells (Kcs), extrahepatic macrophages, neutrophils, hepatic stellate cells, liver sinusoidal endothelial cells, and platelets are involved in the HIRI progress.[2] The released damage-associated molecular patterns activate hepatic macrophages and initiate immune responses.[3]

Hepatic macrophages are the key elements to maintain hepatic homeostasis and repairing hepatic injury. There are mainly 2 kinds of macrophages participating in these processes including resident Kcs and myeloid-derived macrophages.[4] It has been known that both sets of macrophages are critical for modulating immunologic responses in HIRI. Resident-Kcs, which contribute approximately 35% of hepatic cells in adult mice, are originated from yolk sac progenitors, attached to the sinusoidal endothelial layer, to capture the immune signaling molecule in the blood, and starts the initial immune responses in HIRI.[2,5,6] During HIRI, Kcs were depleted in the inflammatory response, and myeloid-derived monocytes were prominently infiltrated into injured liver tissues as a major source of macrophage pool.[4] In mice, resident Kcs are CD11b^{low}, F4/80^{high} and Clec4F$^+$, CD11b$^+$, F4/80$^{intermediate\ (int)}$, and Ly6C$^+$ and CSF1R$^+$ cells were considered as myeloid-derived macrophages.[7–11] However, the molecular mechanism of these 2 subsets, especially myeloid macrophages, in HIRI waits to be further clarified.

The excessive proinflammatory response is considered as the critical factor in aggravating the severity of HIRI. During HIRI, Kcs produce monocyte chemoattractant protein 1 (MCP-1/C-C motif chemokine ligand 2) to recruit monocyte-derived CD11b$^+$Ly6C$^+$CCR2$^+$CX3CR1$^-$ macrophages[12] and necrotic depletion of Kcs often coincides with infiltration/activation of circulating monocyte-derived macrophages to promote proinflammatory immune activation of the liver.[13] After the initial stage of HIRI, the activated platelets interact with monocyte-derived Ly6C$^+$ CCR2$^+$ macrophages via P-selectin, and further stimulate neutrophil activation through releasing soluble CD40L, together with neutrophil extracellular traps and leads to the swelling hepatocytes and liver sinusoidal endothelial cells.[14] In the meantime, phagocytic macrophages uptake apoptotic cells and release transforming growth factor-β and interleukin (IL)-10, which might trigger the anti-inflammatory response.[15] Improving anti-inflammatory function of macrophages has been considered as a potential direction in the treatment of HIRI. Prussian blue scavenger with reactive oxygen species scavenging and anti-inflammatory properties was found to protect liver tissues by activating M2-type polarization of macrophages.[16]

Cell division cycle 42 (Cdc42), a small GTPase, is activated when combined with GTP and inactivated when combined with GDP[17] and plays a role of molecular switch in cell physiological activities.[18] Activated Cdc42 participates in cell polarity, cytoskeleton remodeling, cell adhesion, cell migration, and cell proliferation by regulating P21 (RAC1) activated kinases, myotonic dystrophy kinase-related Cdc42-binding kinases, mixed lineage kinases, and other kinases,[19–22] and Cdc42 deficiency leads to embryonic lethality.[23] Studies have shown that Cdc42 and its downstream proteins, such as ACK1, modulate the proliferation, adhesion, and migration of tumor cells by regulating the JAK/STAT pathway.[17,24–27] *Brucella abortus* activates Cdc42 through TLR4, which leads to the phosphorylation of downstream PI3K and MAPKs after JAK2 in which assist macrophages in phagocytosis of *B abortus*.[28] It has been reported that in the liver cancer cell line Huh7, Cdc42-mediated ACK1 activation phosphorylates signal transducers and activators of transcription (STAT) 1, resulting in upregulation of downstream interferon (IFN) activating gene, so as to inhibit the replication of hepatitis C virus.[29] These studies suggest that Cdc42 might be involved in inflammatory response. However, the role of Cdc42 in the inflammatory response in HIRI remains unknown.

In this study, we examine whether Cdc42 affects the course of HIRI with myeloid-specific deletion of Cdc42 mice and explore the underlying mechanism. Our main findings are that myeloid deficiency of Cdc42 restrained the infiltration of macrophages into liver, suppressed proinflammatory response, enhanced M2 macrophage polarization, and alleviated hepatic necrosis in HIRI. In addition, our results suggest that inactivation of Cdc42 lessened activation of STAT1/suppressor of cytokine signaling (SOCS) 3 and enhanced STAT3 and STAT6 signals in macrophages, in which Cdc42 might function as a key factor in modulating the balance between proinflammatory and anti-inflammatory activity of macrophages during HIRI progression.

Results
Myeloid Cdc42 Deficiency Alleviated HIRI in Mice

To explore the function of Cdc42 in liver, an HIRI model was established with Cdc42^{mye} mice. Our results showed that myeloid-specific deletion of Cdc42 significantly
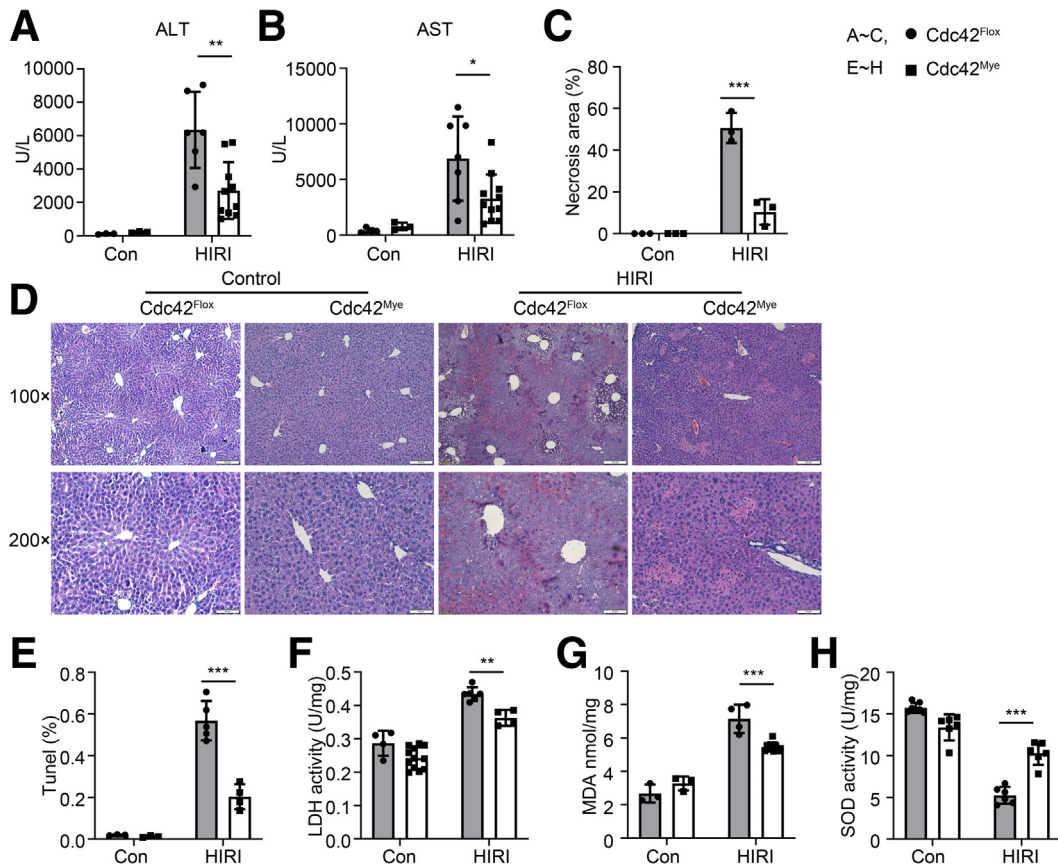
Figure 1. Myeloid deletion of Cdc42 alleviates the liver damages induced by HIRI in mice. Mouse HIRI model was established with 1-hour ischemia followed by 12-hour reperfusion in myeloid Cdc42 knockout (Cdc42[mye]) and wild-type (Cdc42[flox]) mice, N=12 per group. Serum alanine transaminase (ALT) (*A*) and aspartate aminotransferase (AST) (*B*) were measured in HIRI models from Cdc42[mye] and Cdc42[flox] mice, n=3-11 as indicated. Histologic images were taken from hematoxylin-eosin staining in mouse liver tissues with or without HIRI (*C, D*), scale bars = 50 μm, n=3. Apoptotic hepatocytes were determined by 1-step terminal-deoxynucleotidyl transferase mediated nick end labeling (TUNEL) analysis in liver tissues (*E*), n=3-5 as indicated. The lactate dehydrogenase (LDH) activities (*F*), malondialdehyde (MDA) contents (*G*), and superoxide dismutase (SOD) activities (*H*) were measured in liver tissues of mice, n=3-12 as indicated. The results were presented as mean ± standard deviation with at least 3 replicates. *$P < .05$; **$P < .01$; ***$P < .001$.

decreased serum alanine transaminase (Figure 1*A*), and aspartate aminotransferase (Figure 1*B*) levels following HIRI in Cdc42[mye] mice compared with Cdc42[flox] mice. In addition, Cdc42 deficiency remarkably reduced hepatic necrosis, sinusoidal edema, vacuolization (Figure 1*C* and *D*), and apoptosis (Figure 1*E*) in Cdc42[mye] livers in HIRI. Furthermore, Cdc42 deficiency inhibited the activities of lactate dehydrogenase (Figure 1*F*), suppressed the oxidative stress responses with reduction of malondialdehyde (Figure 1*G*), and increased superoxide dismutase activities (Figure 1*H*) in the liver in mice following HIRI. These results indicated that myeloid Cdc42 deficiency protected livers from HIRI in mice.

Myeloid Cdc42 Deficiency Restrained the Infiltration of Myeloid-Derived Macrophages in Liver During HIRI

Myeloid lineage was traced and evaluated with the fluorescent myeloid-derived macrophages in livers in HIRI

models using Rosa mTmG/LyzCre reporter mice (mTmG). The mT/mG mice carry 2-color fluorescent reporters, in which cell membrane-localized tdTomato (mT) fluorescence (red) expression is widespread in cells/tissues before Cre recombination, and then the red fluorescence will be replaced by fluorescent EGFP (mG) (green) in the Cre expressing cells after excising floxed tdTomato (mT)-stop box. The mT/mG mice have been used in cell lineage tracing by crossing with tissue-specific Cre expressing mice as illustrated in Figure 2*A*.[30] The fluorescence of liver cryosections were recorded and analyzed for LyzCre excised EGFP-positive myeloid-derived macrophages from Cdc42[mye]ROSA[mTmG] (Cdc42 ROSA Lyz) and ROSA[mTmG] (Rosa Lyz) mice (Figure 2*B*). In addition, we also performed a CD11b immunofluorescence staining to examine the distribution of infiltrated myeloid macrophages in the paraffin liver sections (Figure 2*C*). The results showed that there were not much myeloid-originated cells in resting livers in both Rosa Lyz and Cdc42 ROSA Lyz mice and myeloid deletion of Cdc42 restrained monocyte/macrophage
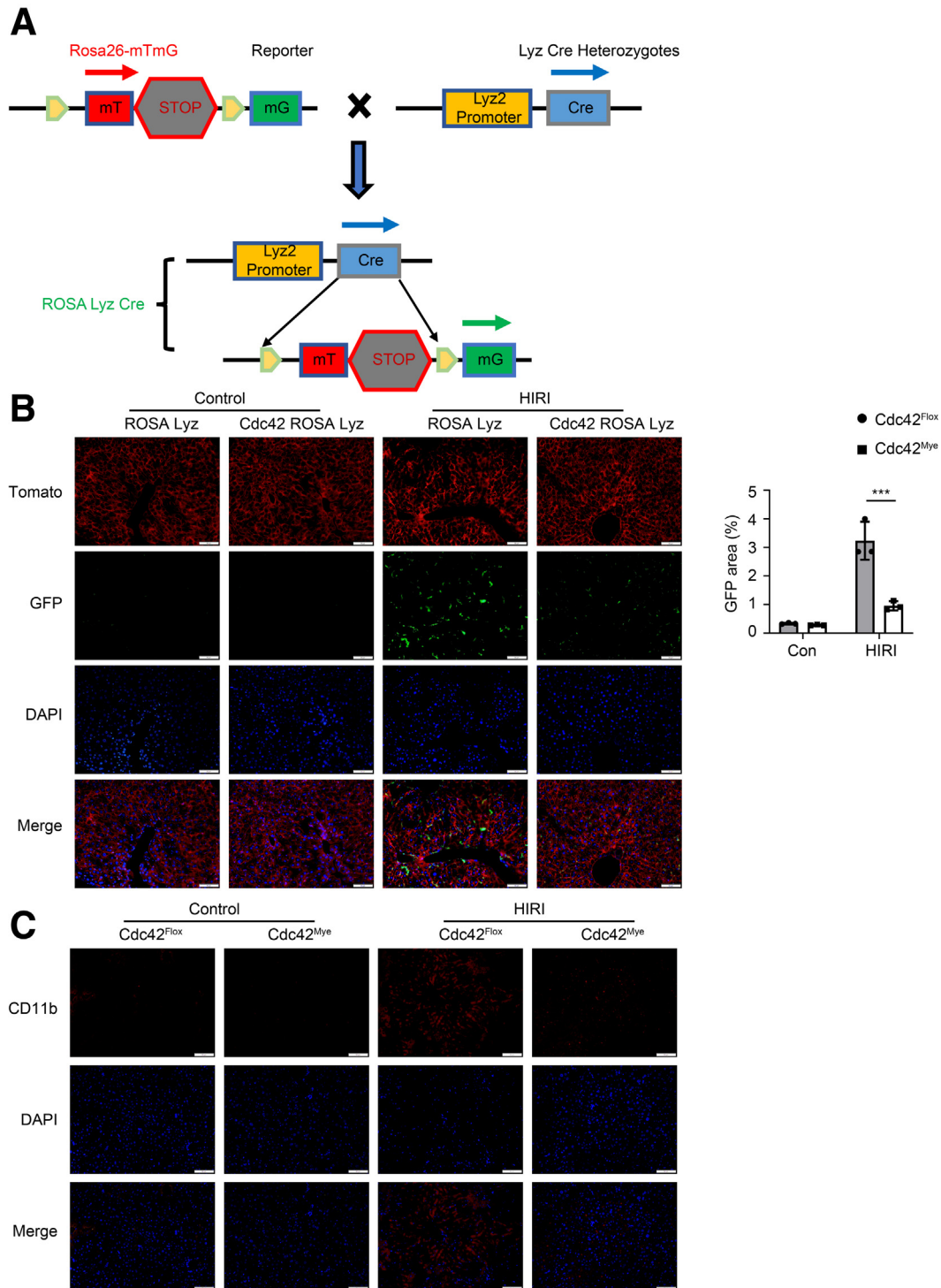
Figure 2. Myeloid deletion of Cdc42 suppressed macrophage infiltration in HIRI liver tissues. Myeloid-derived macrophages are traced by fluorescence with Rosa mTmG reporter in liver tissues in HIRI. A schematic diagram for generation of myeloid Rosa mTmG/LyzCre mice or myeloid Cdc42^{mye}/Rosa mTmG/LyzCre mice, in which LyzCre$^+$ myeloid lineage cells were green fluorescent protein (GFP, mG) positive in *green*, other cells were expressing Tomato fluorescent proteins (mT) in *red* (*A*). Representative fluorescent images of livers from Rosa mTmG/LyzCre mice and Cdc42^{mye}/Rosa mTmG/LyzCre mice were shown (*B*). The hepatic localization of CD11B-positive cells were labeled with immunofluorescence in sham and HIRI mice (*C*). scale bars = 50 μm, n = 3. ***$P < .001$.

infiltration into the liver following HIRI (Figure 2B). The similar results were also observed with immunofluorescent staining with CD11b (Figure 2C). These results indicated that myeloid Cdc42 deficiency suppressed the infiltration of myeloid-derived macrophages in livers, which was triggered by HIRI.

Cdc42 Deficiency Suppressed Macrophage M1 Polarization and Promoted Macrophage M2 Polarization in HIRI Livers in Mice

Next, we tried to determine whether Cdc42 deficiency affects the function of myeloid macrophage in HIRI. A multiplex immunofluorescence (mIF) costaining experiment, based on Tyramide signal amplification method, was performed in liver tissue sections with primary antibodies of CCR2, CD11b, CD86, and CD206 (Figure 3A) or CCR2, CD11b, inducible nitric oxide synthase (iNOS), and CD206 (Figure 3B). It was shown that the infiltrating macrophages were significantly increased with myeloid origin marked by CCR2 and CD11b following HIRI. Furthermore, these infiltrated macrophages were mainly inflammatory M1 macrophages labeled by CD86 or iNOS in Cdc42^{flox} group, and mainly in anti-inflammatory M2-type marked by CD206 in Cdc42^{mye} group (Figure 3A and B).

Myeloid Cdc42 Deficiency Inhibited HIRI-Induced Inflammatory Response in Mice

Blood cell components including white blood cells (WBC), red blood cells, lymphocytes, granulocytes, and intermediate cells (Mid) were examined to evaluate systemic immune response in mice. As shown in Figure 3A–E, there were no significant differences in numbers of the blood cell components between Cdc42^{mye} and Cdc42^{flox} mice in the resting condition. However, HIRI significantly reduced the numbers of WBC and lymphocytes, and increased the number of granulocytes, although there were no alterations in red blood cells and Mid cells, whereas myeloid Cdc42 deficiency slightly enhanced the total number of WBCs and lymphocytes and decreased the proportion of Mid cells in HIRI mice (Figure 4A–E). These results indicated that myeloid deletion of Cdc42 might play a role in innate immune response and peripheral blood cell distribution. To further examine the effects of Cdc42 in myeloid-derived cells in blood cell distribution, we performed flow cytometry assays (FCA) in mouse whole blood cells following HIRI. The neutrophile granulocytes (neutrophils) were marked by CD11b$^+$Ly6G^{High}Ly6C^{Low}, and the monocytes were marked by CD11b$^+$Ly6G^{Low}Ly6C^{High}. The results showed that myeloid Cdc42 deficiency did not alter the proportion of neutrophils (Figure 4F and G), but relatively reduced the proportion of monocytes (Figure 4F and H) in mouse blood in HIRI model.

The expression or secretion of cytokines is also essential for evaluating the inflammatory response in HIRI. Mouse cytokine antibody array or real-time quantitative polymerase chain reaction (qRT-PCR) were performed in the serum or liver tissues in mouse following HIRI, respectively. The results showed that HIRI significantly increased the hepatic expressions of proinflammatory cytokines tumor necrosis factor (TNF)-α, IL1β, and IL6, which were significantly reduced in Cdc42^{mye} mice and myeloid Cdc42 deficiency increased the expression of anti-inflammatory protein CD206 in liver tissues in mouse HIRI models (Figure 4I–L). In addition, mouse cytokine antibody array showed that myeloid Cdc42 deficiency reduced the secretions of proinflammatory cytokines including MCP-1, IL6, TNF-α, and IFN-γ, but enhanced the secretion of anti-inflammatory cytokines, such as IL13 and sTNFR1, in mouse sera in HIRI models (Figure 4M and N). These results indicated that myeloid Cdc42 deficiency suppressed proinflammatory immune responses in HIRI mice.

Myeloid Cdc42 Deficiency Enhanced Anti-inflammatory Effects and Facilitated Macrophage M2-Type Polarization in HIRI Mice

CD206 (mannose receptor 1, Mrc1) is highly expressed in alternatively activated macrophages and is considered as a marker for M2 polarization. To further explore whether Cdc42 has an impact on polarization of myeloid macrophages in HIRI, immunohistochemistry staining of CD206 was performed in liver tissues. Our results showed that the CD206$^+$ cells were increased and mainly located in the hepatic sinusoid, which resembled the infiltrated sites of myeloid macrophages in HIRI livers, and myeloid deletion of Cdc42 increased the numbers of CD206$^+$ macrophages in HIRI liver (Figure 5A). Because cytokines were mostly produced and secreted by macrophages, the protein levels of cytokines IL6, IL10, iNOS, and arginase 1 (ARG1) were also examined in liver tissues. The results showed that the expressions of IL6 and IL10 were significantly increased in HIRI livers and myeloid deletion of Cdc42 remarkably reduced the expressions of IL6 and IL10 (Figure 5B–D), reduced the expressions of iNOS, the marker of M1-type macrophage, and enhanced the expressions of ARG1, the marker of M2-type macrophage (Figure 5B, E, and F). Moreover, an FCA for WBCs was performed by sorting Ly6C$^+$CD11b$^+$ cells (Figure 5G) and followed by selecting CD86 or CD206 positive cells. The results showed that the proportion of Ly6C$^+$CD11b$^+$ monocytes with high CD86 expression was suppressed, whereas the proportion of Ly6C$^+$CD11b$^+$CD206$^+$ cells was relatively increased in myeloid Cdc42 deficiency mice following HIRI (Figure 5G). Therefore, it suggested that myeloid deletion of Cdc42 suppressed proinflammatory and promoted anti-inflammatory effects via modulating macrophage polarization to prevent HIRI in vivo.

Cdc42 Participated in Macrophage Polarization and Myeloid Cdc42 Deficiency Suppressed M1-Type Macrophage Polarization In Vitro

Macrophages have the flexible ability to alter their polarization phenotypes in response to local environmental changes and secrete different cytokines in immune response. Classical in vitro experiments were designed to confirm the effect of Cdc42 in macrophage polarization with
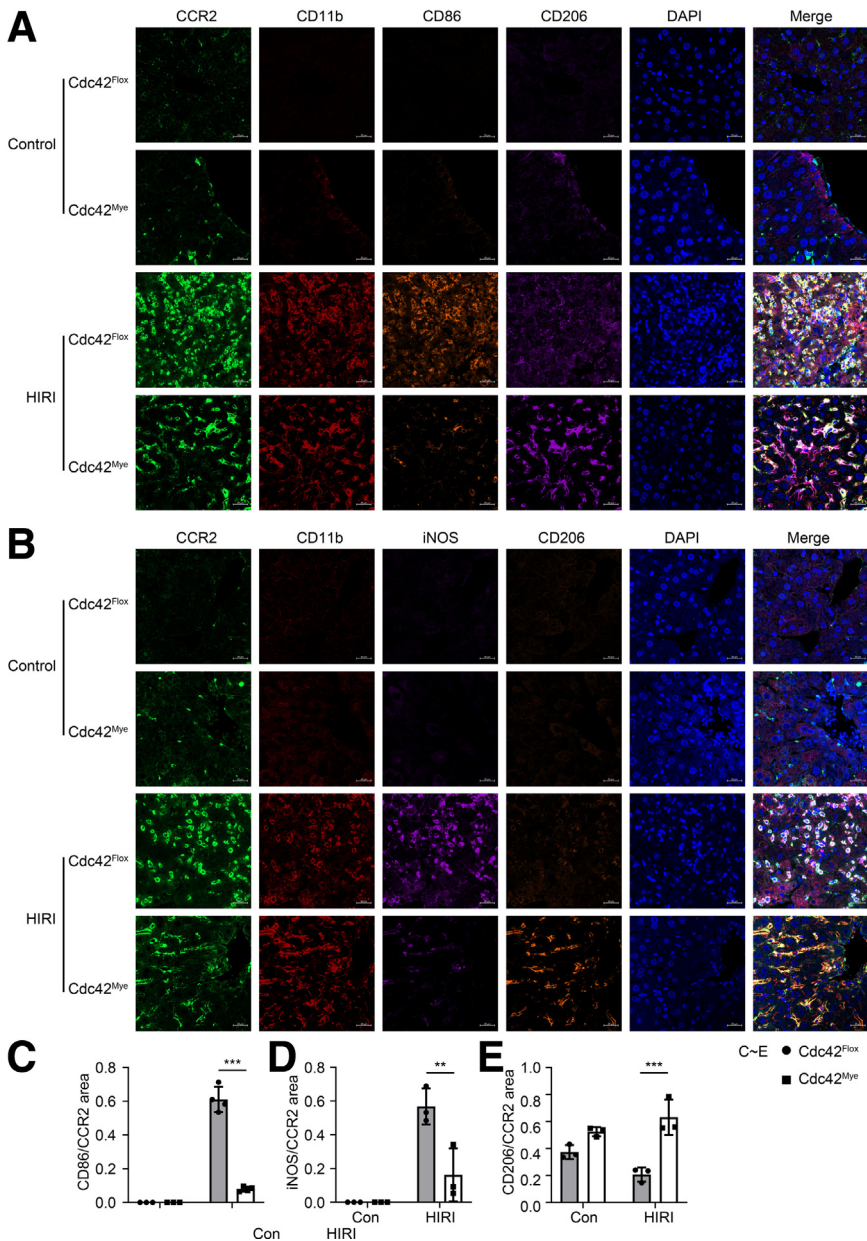
Figure 3. Cdc42 deficiency suppressed macrophage M1 polarization and promoted macrophage M2 polarization in HIRI livers in mice. An mlF experiment, based on tyramide signal amplification method was performed with CCR2, CD11B, CD86, and CD206 (*A, C, E*) or CCR2, CD11B, iNOS, and CD206 (*B, D*) on HIRI liver tissue sections in myeloid Cdc42 knockout (Cdc42^{mye}) and wild-type (Cdc42^{flox}) mice. scale bars = 20 μm, n=3, **$P <$ 0.01; ***$P <$ 0.001.

proinflammatory stimuli, such as lipopolysaccharides (LPS)/LPS+ IFN-γ for M1 polarization, or IL4/IL4 + IL13 for M2-type polarization. Bone marrow–derived macrophages (BMDMs) from Cdc42^{flox} or Cdc42^{mye} mice were isolated and induced with macrophage colony–stimulating factor. Under LPS (100 ng/mL, 24 hours) stimulation, the secretions of cytokines and chemokines, such as sTNFR1, MCP-5, MCP-1, regulated on activation normally t-expressed and presumably secreted, IL12, and IL6, which are mostly indicated as proinflammatory status, were increased, and Cdc42 deficiency decreased the secretions of IL6, IL12, and MCP-1; whereas under IL4 (40 ng/mL, 48 hours) stimulation, only MCP-5, MCP-1, and sTNFR1 were increased and Cdc42 deficiency slightly enhanced the secretion of MCP-1 (Figure 6*A–C*) from BMDMs.

With ML141, a specific inhibitor of Cdc42, we further evaluated the role of Cdc42 in macrophage polarization in 2 different sources of monocyte cell lines (Raw264.7 and Thp1) under the stimulation of LPS (100 ng/mL) and IFN-γ (20 ng/mL, for M1-type polarization), or IL4 + IL13 (both at 40 ng/mL, for M2-type polarization). Suppression of Cdc42 reduced the LPS stimulated expressions of IL6, TNF-α, and IL1β in RAW264.7 cells, a mouse monocyte cell line (Figure 6*D–F*). In addition, the mRNA expression of SOCS3, which is a STAT1-regulated suppressor of STATs family and plays a critical role in promoting M1 polarization,[31] was suppressed in the presence of ML141 (Figure 6*G*).

Moreover, the mRNA expressions of IL1β, CD86, MCP-1, SOCS3, and TNF-α were also decreased in Cdc42^{mye} peritoneal macrophages compared with Cdc42^{flox} group under
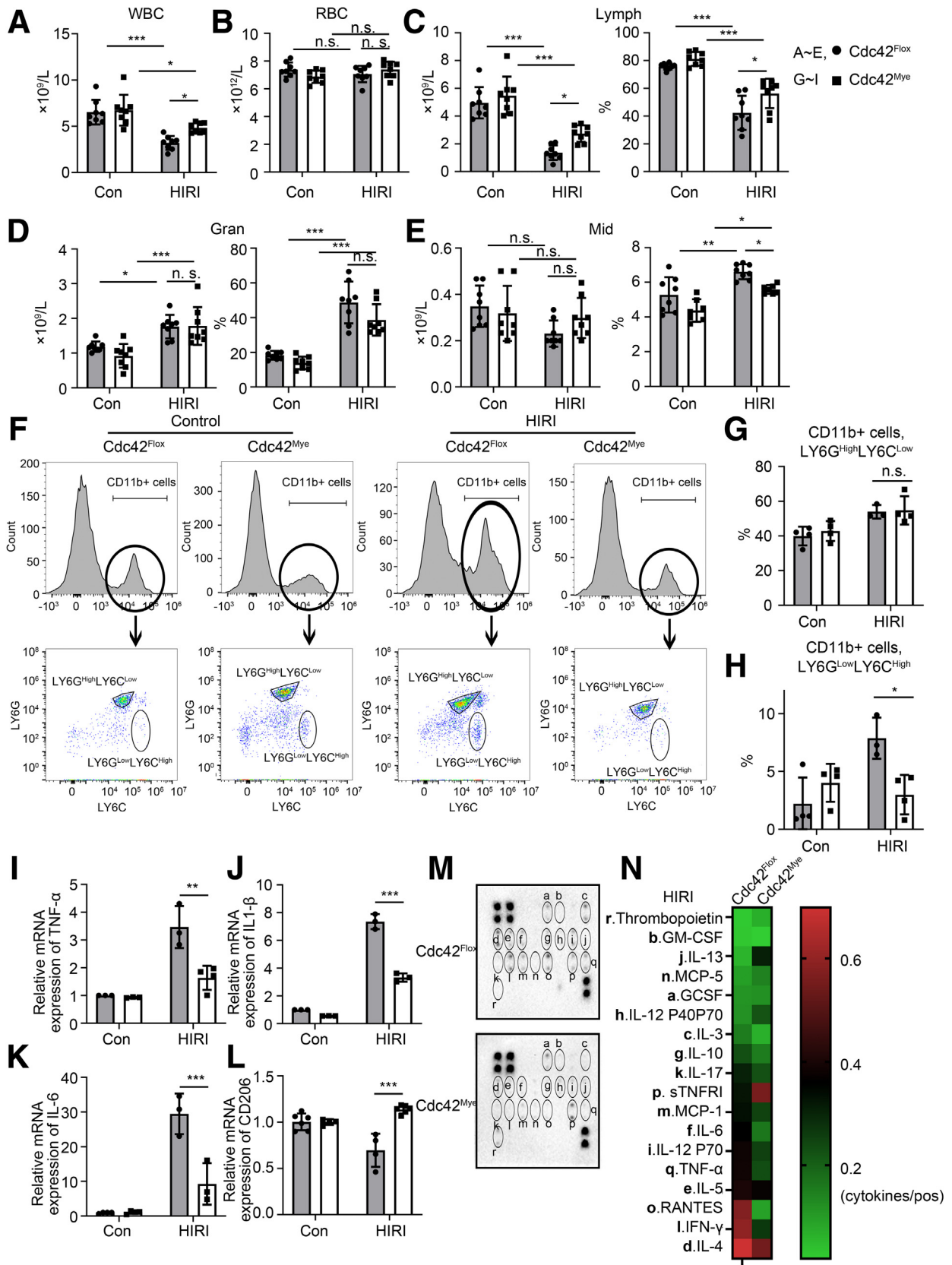
Figure 4. Myeloid deletion of Cdc42 inhibits HIRI-induced inflammatory response in mice. Blood cell components such as WBC (A), red blood cell (B), lymph (C), granulocytes (Gran) (D), and Mid (E) were examined by routine blood analysis, n=7-8 as indicated. FCA was performed with CD11b, Ly6C or Ly6G labeling in blood cells (F–H), n=3-4 as indicated, and the mRNA expressions of TNF-α (I), IL1β (J), IL6 (K), and CD206 (L) were determined by qRT-PCR analysis in liver tissues, n=3-6 as indicated. Mouse serum cytokines (M, N) were detected with mouse cytokine antibody array in HIRI models from Cdc42^{mye} compared with Cdc42^{flox} mice. n. s., no significance; *$P < .05$; **$P < .01$; ***$P < .001$.
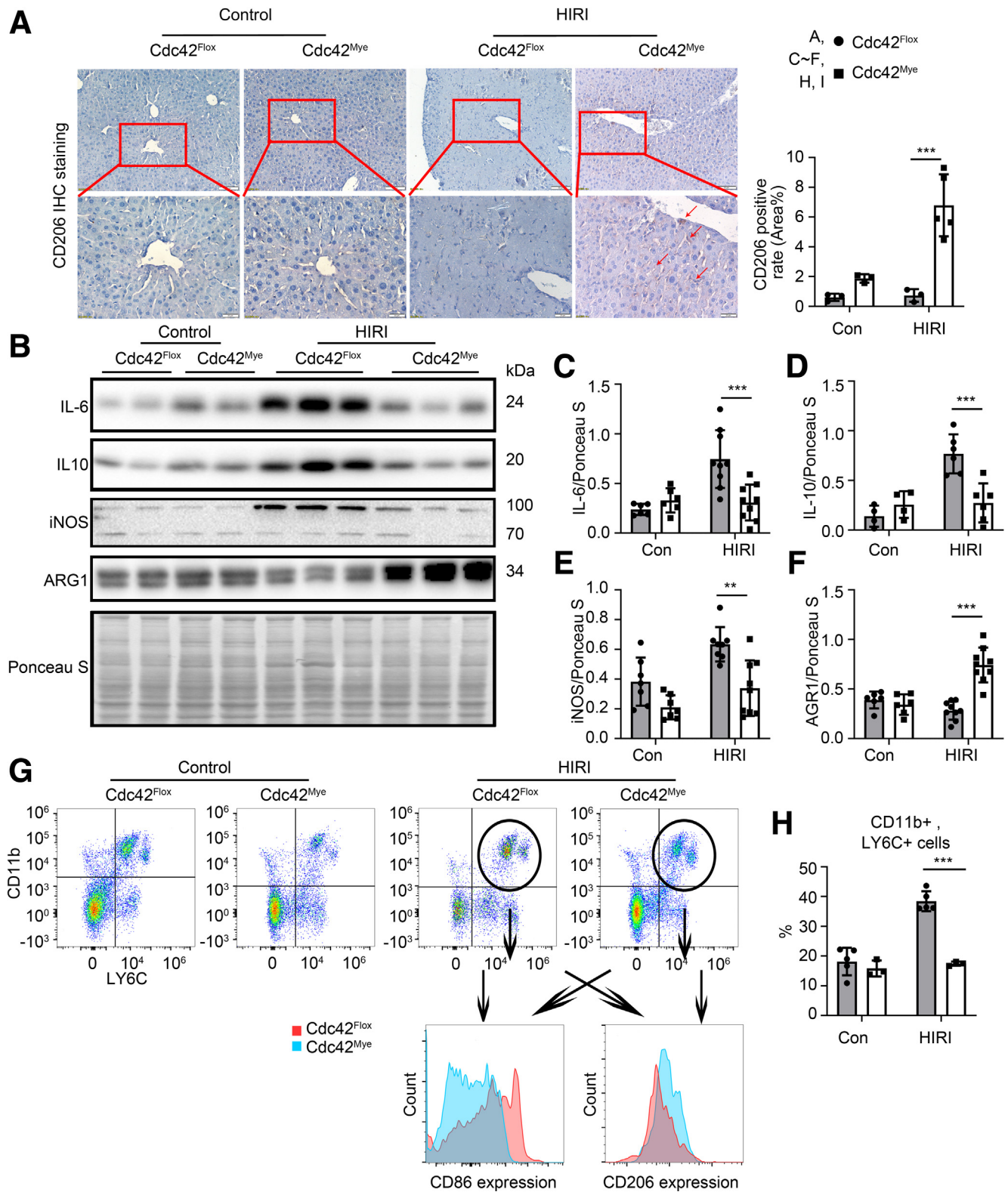
Figure 5. Myeloid deletion of Cdc42 facilitates M2-type polarization of macrophages in HIRI model of mice. Expressions of CD206 were determined by immunohistochemical staining analysis with antibody against CD206 in liver tissues of Cdc42[mye] and Cdc42[flox] mice, scale bars = 50 μm or 20 μm as indicated, respectively (*A*), n=3-5 as indicated. The images (*B*) and quantitative results of IL6 (*C*), IL10 (*D*), iNOS (*E*), and ARG1 (*F*) were analyzed by Western blot assay in mouse liver tissues, n=4-9 as indicated. FCA of Ly6C, CD11b, CD86, and CD206 labeling in blood cells for M1/M2 macrophage typing were performed (*G*, *H*), n=3-5 as indicated. **$P < .01$; ***$P < .001$.
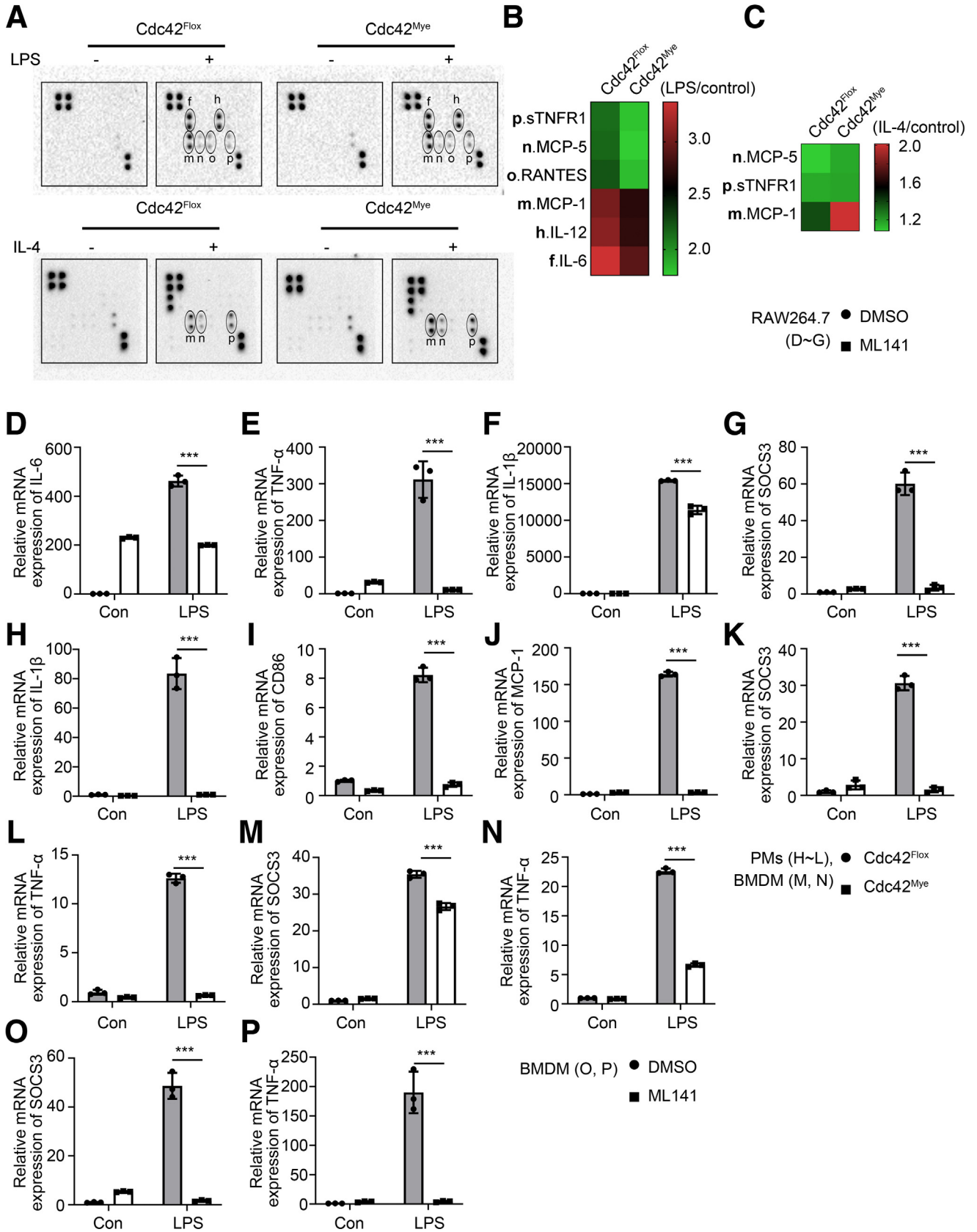
LPS stimulation (Figure 6H–L). Similar results also occurred in BMDMs from Cdc42[mye] and Cdc42[flox] mice (Figure 6M and N), or in BMDMs, which Cdc42 was inactivated by a specific inhibitor ML141 (Figure 6O and P). These results indicated that Cdc42 plays a critical role in macrophage polarization and myeloid deficiency of Cdc42 suppressed M1 polarization and proinflammatory response and might enhance M1 to M2 switch under inflammatory condition.

In addition, under pretreatment with ML141, the polarization state of THP1, a human monocyte cell line, was determined by FCA with labeling of CD11b-APC (as the marker for macrophages), CD86-FITC or CD64-FITC (for M1 macrophages), and CD206-FITC (for M2 macrophages). The results showed that inhibition of Cdc42 activities reduced CD86 and CD64 expression for M1-type polarization and enhanced CD206 expression for M2-type polarization (Figure 7A–C).

Inhibition of Cdc42 Promoted Anti-inflammatory Effects through STATs-SOCSs Signaling Pathway in Macrophage Polarization

STAT family is known as an information exchange center for macrophage polarization and often activated by various cytokines. STATs are closely interacted with SOCS proteins, which negatively regulate JAK/STAT signaling via feedback loop to regulate polarization of macrophages and mediate cytokine signals.[32,33] For example, IL6-mediated STAT3 activation was inhibited by SOCS3, which is prominently induced by LPS or other proinflammatory molecules, such as TNF, to sustain inflammatory response in macrophages.[34] It has been known that Cdc42 and other Rho GTPases have been implicated in STAT activation in cancer cells.[24] Here, we further explored the interaction between Cdc42 and STATs-SOCSs signaling in macrophages. In the presence of ML141, the phosphorylation level of STAT1 and the expression of SOCS3 in THP-1 cells were significantly reduced, whereas the phosphorylation of STAT3 was enhanced after LPS and IFN-γ stimulation (Figure 8A, C, D, and F). Under IL4 and IL13 stimulation, ML141 significantly enhanced the phosphorylation of STAT6 in THP-1 cells (Figure 8A and E). Meanwhile, mouse BMDMs were harvested and induced for M1 or M2 polarization under the treatment of ML141 and the similar results were observed as Thp1 (Figure 8B and G–J). These results indicated that inactivating Cdc42 reduced STAT1 activation and SOCS3 expression and promoted STAT3 and STAT6 activation to direct macrophage polarization toward anti-inflammatory state.

Inhibition of Cdc42 Protects Mice from HIRI

To determine whether inhibition of Cdc42 might provide a protective role in HIRI in vivo, we applied ML141 via peritoneal injection at 10 mg/kg in 12 hours interval twice before HIRI surgeries in mice as described previously. The results showed that inhibition of Cdc42 remarkably reduced HIRI-induced hepatic injury (Figure 9A and B). The infiltration of monocyte-derived macrophages was significantly inhibited with reduction of CCR2 and CD11b macrophages and the inflammatory M1 macrophages with CD86 labeling were reduced, whereas M2 macrophages marked by CD206 were relatively increased in HIRI livers through mIF staining (Figure 9C). These results indicated that inhibition of Cdc42 before hepatic ischemia reperfusion condition might protect the liver from HIRI, which resembled the observations in myeloid Cdc42 deficiency mice.

Discussion

Excessive proinflammatory response following hepatic ischemia-reperfusion is often characterized with the recruitment of myeloid leukocytes and the cascade of proinflammatory mediators, and contributes to HIRI and results in severe liver damage and hepatic malfunction.[35] During HIRI progress, the monocyte-derived macrophages are selectively accumulated in liver tissues to form a proinflammatory microenvironment and secret proinflammatory cytokines, such as TNF-α, to directly cause liver injury.[2] It has been reported that inhibiting macrophage proinflammatory M1 polarization or enhancing anti-inflammatory M2 polarization might play a reparative role in HIRI.[36,37] In this study, we demonstrated that myeloid-specific Cdc42 deletion restrained myeloid monocyte/macrophage infiltration, suppressed proinflammatory responses, promoted macrophage M2 polarization, mitigated hepatic necrosis and reactive oxygen species injury, and reserved hepatic function in mice.

The increased infiltration of monocyte-derived macrophages is the prominent feature of liver injury in HIRI.[38] With Rosa mTmG reporter mice and subsequent LyzCre-mediated excision, we were able to trace fluorescent EGFP-positive myeloid-derived cells in the mouse livers following HIRI (Figure 2A and B). Indeed, GFP-positive myeloid-derived macrophages were likely absent in resting livers and prominently increased in HIRI liver, especially in the area of hepatic sinusoids, which were also confirmed by immunostaining with myeloid-macrophage marker CD11b, and Cdc42 deficiency reduced the infiltration of myeloid macrophages in HIRI liver (Figure 2B and C).

Figure 6. (*See previous page*). **Myeloid deletion of Cdc42 reduces the releases of inflammatory cytokines in macrophages in vitro.** BMDMs were isolated from Cdc42[mye] and Cdc42[flox] mice. Mouse cytokines were determined by mouse cytokine antibody array with the culture medium of the mouse BMDMs stimulated with LPS (100 ng/mL) for 24 hours (A, B), or IL4 (40 ng/mL) for 48 hours (A, C), respectively. The mRNA expressions of IL6, TNF-α, IL1β, and SOCS3 were examined by qRT-PCR analysis in RAW264.7 cells, in which the cells were pretreated with ML141 (10 μM), a Cdc42 suppressor, for 2 hours, and then stimulated with LPS (100 ng/mL) for 6 hours (D–G), n=3. The mRNA expressions of IL1β, CD86, and MCP1 in mouse PMs (H–J) with LPS 100 ng/mL for 12 hours, n=3. The expressions of SOCS3 and TNF-α were detected by qRT-PCR with LPS (100 ng/mL) for 12 hours in mouse PMs (K, L) and BMDMs from myeloid Cdc42 knockout (Cdc42[mye]) and wild-type (Cdc42[flox]) mice (M, N), or BMDMs pretreated with 10 μM ML141 for 2 hours, and stimulated with LPS (100 ng/mL) for 12 hours, respectively (O, P). n=3. ***P < .001.
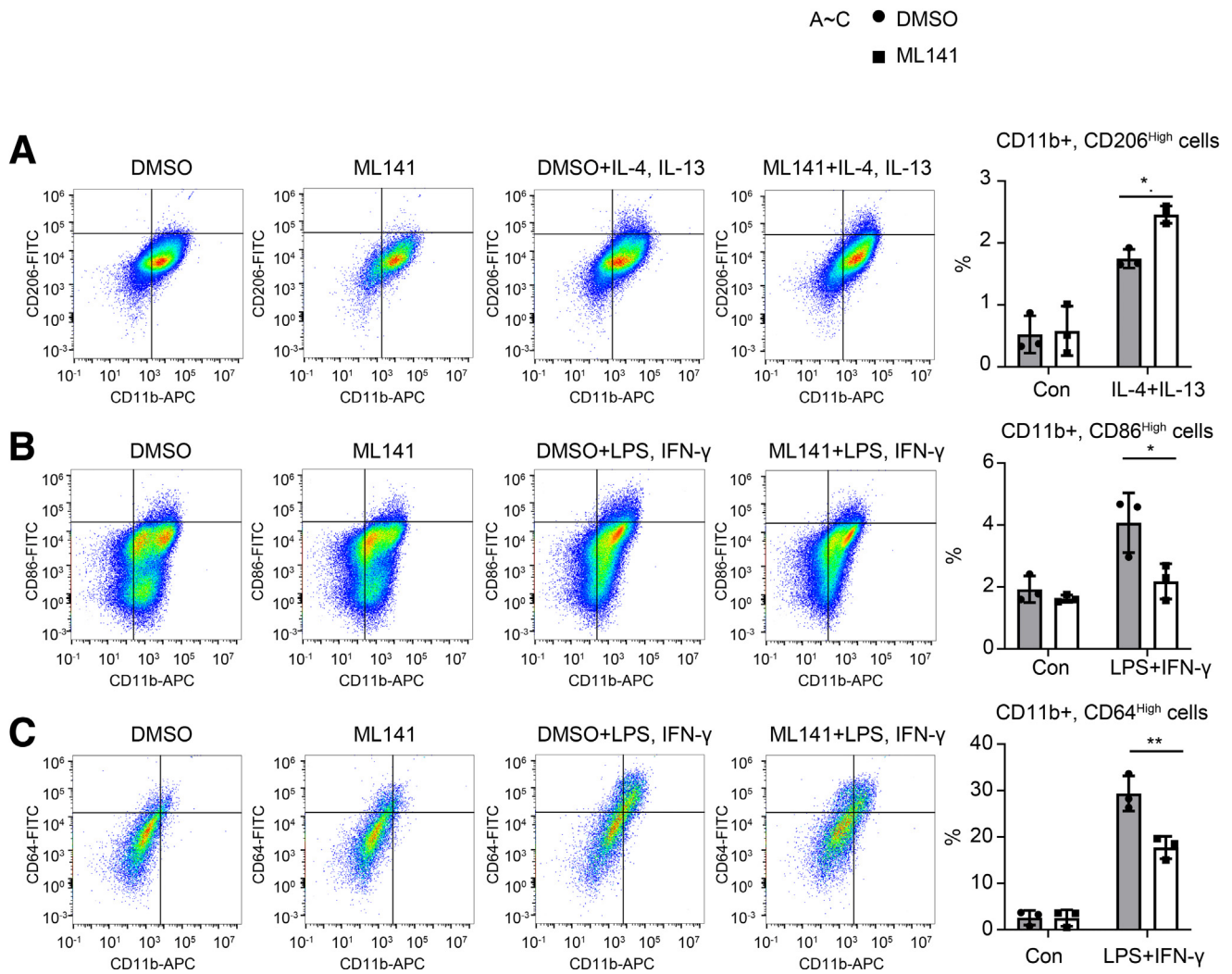
Figure 7. Cdc42 suppression participated in macrophage polarization of THP1. Differentiation of THP1 cells were determined by FCA, in which the cells were labeled with antibodies of CD11b-APC/CD206-FITC, CD11b-APC/CD86-FITC, or CD11b-APC/CD64-FITC, respectively (A–C). THP1 cells were differentiated with PMA 100 ng/mL for 24 hours, then the cells were pretreated with 10 μM ML141 for 2 hours, and further stimulated with LPS (100 ng/mL) and IFN-γ (20 ng/mL) for 24 hours, or IL4 and IL13 (both 40 ng/mL) for 48 hours. n=3. *$P < .05$; **$P < .01$.

Macrophages have the flexible adaptive properties to modulate their phenotype according to local environment, but it is largely unknown how macrophages participate in the process of adaptation, especially in HIRI. Generally, M1 macrophage polarization resembles proinflammatory status, and M2 macrophage polarization is known as an alternatively activated status for anti-inflammation[39] for resolving inflammation, tissue repairing, and remodeling.[40] It is also known that the M2 macrophage polarization ameliorates HIRI by counteracting proinflammatory effects of M1 macrophages.[36,37] Deficiency or inhibition of Cdc42 suppressed M1 and promoted M2 polarization, which was confirmed by CD11b, CD86, iNOS, and CD206 mIF (Figures 2, 3, and 9) in HIRI livers. With ML141 pretreatment before hepatic ischemia reperfusion surgeries, we also found inhibition of Cdc42 activity remarkably blocked the infiltration of myeloid-derived macrophages and alleviated HIRI

(Figure 9), which resembled the protective effects of myeloid Cdc42 deficiency in mice.

The uncontrolled M1 polarization is deleterious to the host, leading to excessive inflammation, tissue damage, and multiple organ failure.[41] STAT family proteins act as the information hub for macrophage polarization-mediated cytokine signals and regulating proinflammatory or anti-inflammatory responses through feedback interactions with SOCS proteins, which are also named as STAT-induced-STAT inhibitor.[32,33] STATs family composes seven members of transcription factors that are mostly ubiquitously expressed except STAT4, and they convert external stimulation signals into different polarization directions of macrophages, by the balance of the interacting regulation between STAT1 and STAT3/STAT6, so as to participate in M1 and M2 polarization.[32] The activation of STAT proteins with tyrosine phosphorylation promotes the formation of
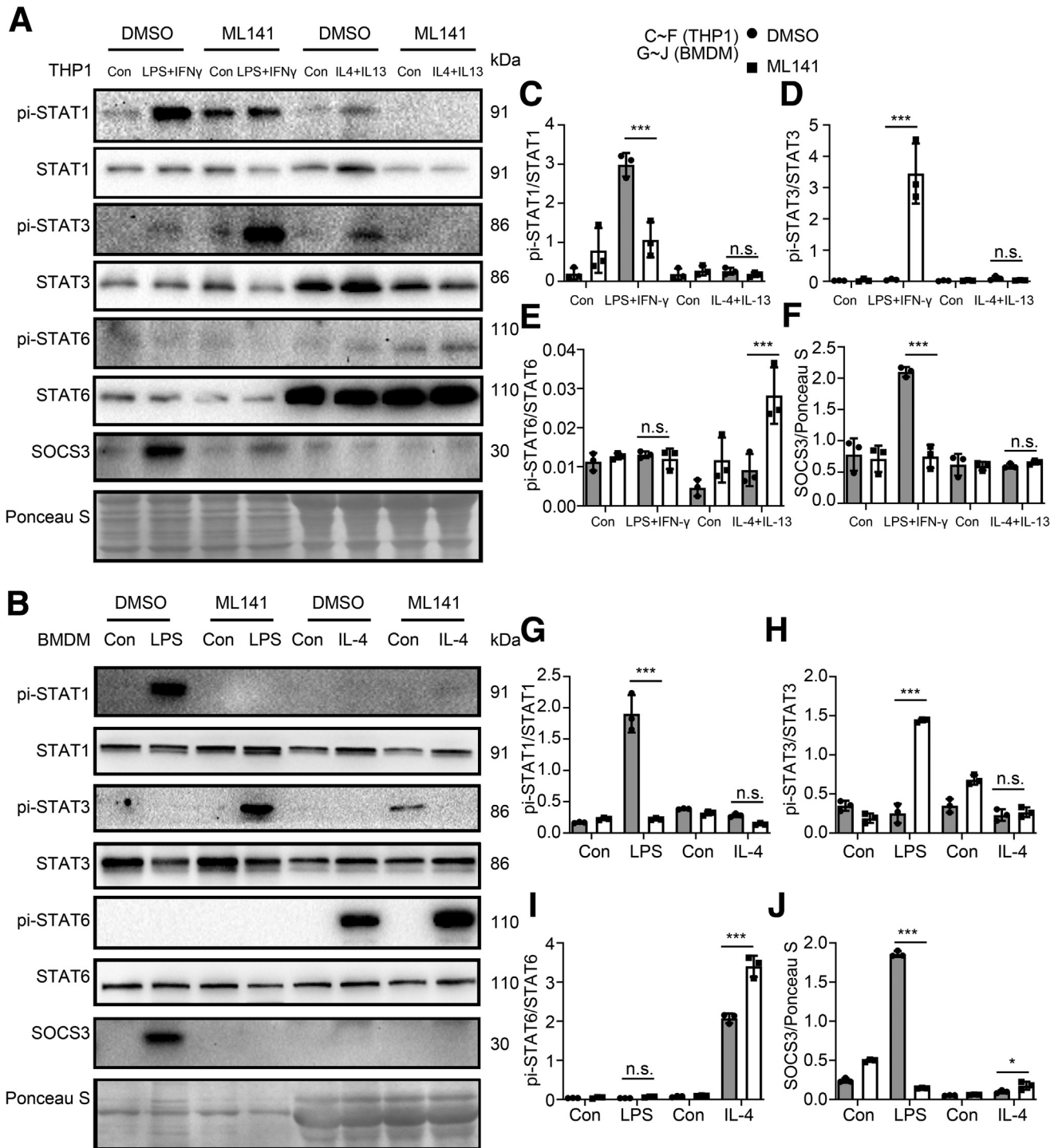
Figure 8. Myeloid deletion of Cdc42 enhances the M2-type differentiation of macrophages via regulating STATs signaling. THP1 cells were pretreated with PMA (100 ng/mL) and ML141 (10 μM) for differentiation and then stimulated with LPS (100 ng/mL) and IFN-γ (20 ng/mL) for 1 hour for M1 induction, or IL4 and IL13 (both at 40 ng/mL) for 48 hours for M2 induction. The images (*A*) and quantitative results (*C–F*) of the phosphorylation of STAT1, STAT3, and STAT6 and expressions of SOCS3 were detected by Western blot analysis in THP1 cells, n = 3. The images (*B*) and quantitative results (*G–J*) of the phosphorylation of STAT1, STAT3, and STAT6 and expressions of SOCS3 were measured by Western blot analysis in BMDMs stimulated with LPS (100 ng/mL) for 3 hours or IL4 (40 ng/mL) for 48 hours, respectively, n = 3. n. s., no significance; *$P < .05$; ***$P < .001$.
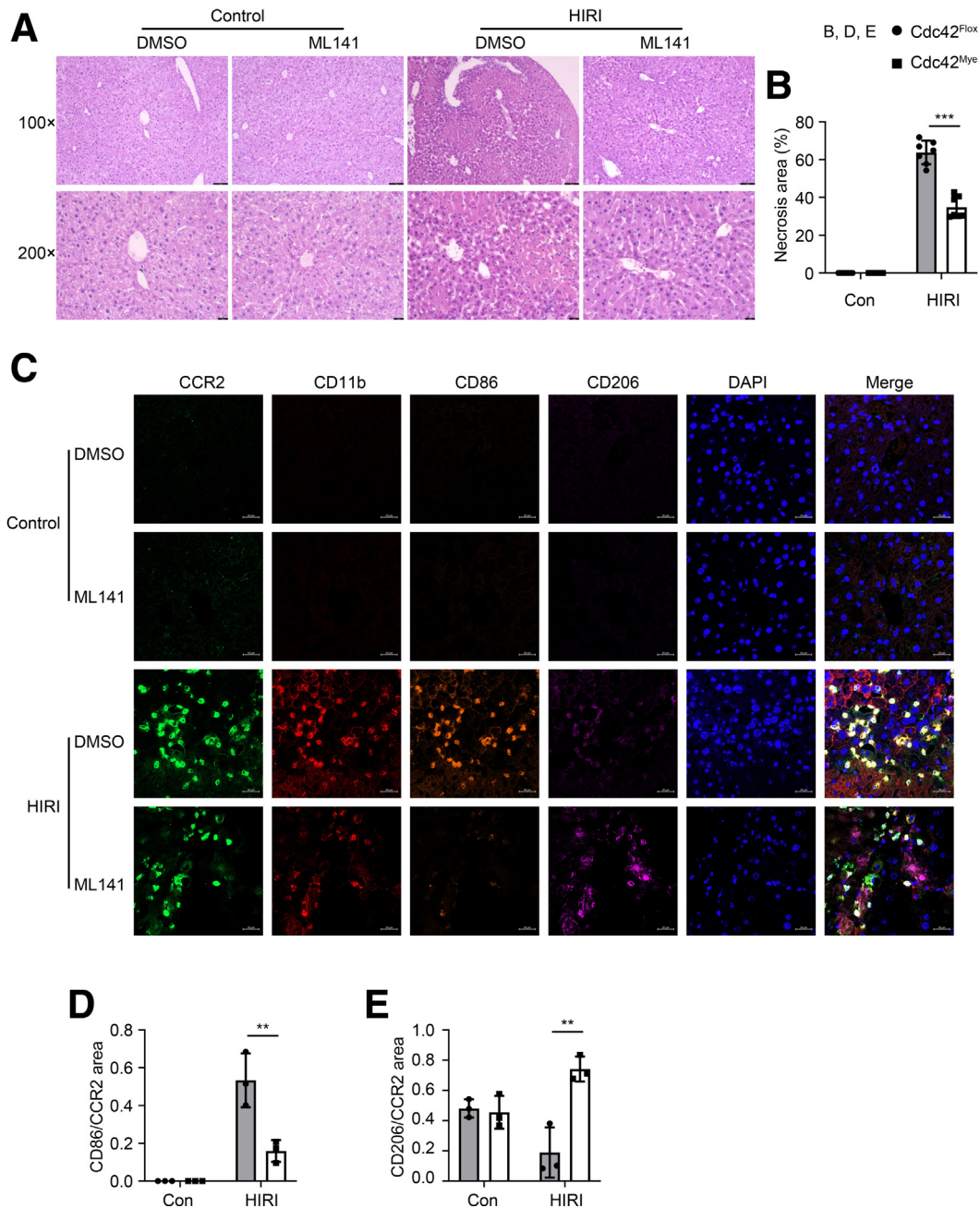
Figure 9. Inhibition of Cdc42 with ML141 protects mice from HIRI. Cdc42 specific inhibitor ML141 was prepared in a sterilized injection solution (2% DMSO+30% PEG 300+5% Tween 80), and administered intraperitoneally to C57/BL6 mice at a dose of 10 mg/kg. Mouse HIRI model was performed 24 hours later as previously described. Hepatic histologic images were taken and analyzed from at least 3 mice per group with or without ML141 injection (*A, B*), scale bars at 75 or 25 μm, n=3. The mIF experiment, based on Tyramide signal amplification method (TSA) was performed with CCR2, CD11b, CD86, and CD206 on liver tissue sections (*C*), n=3. scale bars = 20 μm, **$P < 0.01$; ***$P < .001$.

homodimers or heterotrimers, which translocate into the nucleus to initiate the expressions of target genes. Activation of STAT1 is essential for M1 polarization resulting in cytotoxic and tissue-damage proinflammatory functions, whereas STAT3 and STAT6 are major transcriptional factors responsible for M2 polarization promoting resolution of inflammation and tissue repairing.[32] The activation of STAT3/STAT6, which often were phosphorylated by cytokines IL6 or IL10, inhibits the activation of STAT1, which in turn switches the proinflammatory M1-type polarization toward M2 polarization.[32,34,42] The cytokine-induced SOCSs proteins inhibit phosphorylation of JAK/STATs to balance the proinflammatory and anti-inflammatory response via negative feedback loop.[33] SOCS3 is the important negative regulator for IL6-STAT3 signal, absence of SOCS3 promotes sustained

phosphorylation of STAT3 and an anti-inflammatory response in macrophages.[43] It is known that SOCS3 is strongly upregulated by LPS via activated STAT1.[44] It has been shown that Cdc42-STAT3 signaling axis plays an important role in cell cycle progression in cancer cells.[24,45] However, the effects of Cdc42 on STAT proteins in macrophage activation or polarization has not been revealed.

In this study, we found that absence or inactivation of Cdc42 suppressed M1 polarization and the expressions of proinflammatory cytokines (Figure 6), impaired the phosphorylation of STAT1 (at Tyr701), and reduced the expression of SOCS3 (Figures 6G, K, M, and O, and 8A–C, F, G, and J) in mouse BMDMs and additional independent monocyte cell lines RAW264.7 and THP1, respectively. Studies have showed that the absence of SOCS3 would lead to a long-lived phosphorylated STAT3 via IL6.[43,46] It might explain the enhanced activation of STAT3 (at Tyr705) because of the reduced expression of SOCS3 under LPS/LPS + IFN-γ stimulation in Cdc42 suppressed BMDMs/THP1 cells (Figure 8A, B, D, and H). On inactivation of Cdc42, the phosphorylation of STAT6 (at Tyr641) was increased in THP1 under the stimulation of IL4 + IL13 (Figure 8A and E). Therefore, Cdc42 deficiency or inhibition might promote M1 to M2 switch to reduce the expressions and secretions of proinflammatory cytokines and favoring M2 polarization, as seen in Figure 7 in macrophages. Therefore, myeloid Cdc42 deficiency or inactivation suppresses proinflammatory response and directs macrophage polarization toward the M2-type direction via downregulating STAT1-SOCS3 signal axis and promoting STAT3 and STAT6 activation. It suggested that Cdc42 might be the key modulator for M1-M2 polarization switches in macrophages via modulating STATs signaling.

In summary, myeloid Cdc42 deficiency attenuates HIRI via suppressing proinflammatory response through restraining the infiltration of myeloid macrophages and enhancing M1 to M2 polarization switch via suppressing STAT1-SOCS3 signaling axis and promoted STAT3/STAT6 activation. Understanding and eventually harnessing this mechanism might provide fresh ideas or options in alleviating HIRI.

Methods
Animal Strains and Genotyping
Myeloid Cdc42 knockout (Cdc42[mye]) were generated by crossing Cdc42[flox] with LyzCre mice,[47] and were maintained in C57BL/6 background for at least 5–8 generations. ROSA[mTmG]Lyz mice were obtained by crossing ROSA[mTmG] mice[30] with LyzCre mice, and Cdc42[mye]ROSA[mTmG] mice were obtained by crossing ROSA[mTmG]Lyz and Cdc42[flox] mice.[48] Male mice at 8–12 weeks old were used in the experiments. The genotyping primers were presented as F$_{Cdc42Fl}$ (5′-TGCCTCTACCTCCTAAGTGCTGGGA-3′) and R$_{Cdc42Fl}$ (5′-AGAGGACCCTTACAGGCCTCTTCCA-3′) for Cdc42-flox, F$_{Cre}$ (5′-GACCAGGTTCGTTCACTCA-3′) and R$_{Cre}$ (5′-ACCAGAGTCATCCTTAGCG-3′) for Cre, F$_{Rosa}$ (5′-CTCTGCTGCCTCCTGGCTTCT-3′), R$_{Rosa}$ (5′-CGAGGCGGATCACAAGCAATA-3′) and R$_{RosaM}$ (5′-TCAATGGGCGGGGGTCGTT-3′) for ROSA[mTmG].

All animal experimental protocols were reviewed and approved by the Animal Care and Use Committee of Nanchang University.

HIRI Modeling
HIRI modeling was performed as described.[49] Briefly, mice were anesthetized with isoflurane gas after 6 hours' fasting. The portal vein, hepatic artery, and bile ducts were carefully exposed and clamped with vascular clip for 1 hour to block blood circulation for an area in the middle and left lobes of liver (approximately 70% of the liver), the blood flow was restored by removing the clip. The mice were euthanized after reperfusion for 12 hours with isoflurane anesthetizing and CO_2 inhalation to collect blood and tissue samples.

Evaluation of Hepatic Function
Hepatic function was evaluated by measuring the contents of serum alanine transaminase and aspartate aminotransferase by the technology service of Servicebio company (Wuhan, PR China). The contents of malondialdehyde, superoxide dismutase, and lactate dehydrogenase in liver were measured with the assay kits (Nanjing Jiancheng Bioengineering Institute, A003-1-2, A001-3-2, A020-2-2) according to the manufacturer's protocol.

Histology and Immunostaining
The tissues were fixed in 4% paraformaldehyde in phosphate-buffered saline for overnight and embedded in paraffins. The tissue sections were cut at 4 μm and dewaxed in xylene and rehydrated in serial ethanol solution (100%, 95%, 75%, 50%, and 30% ethanol) and ddH$_2$O. Then, the sections were stained with hematoxylin and eosin, or permeabilized with proteinase K 1 mg/mL in phosphate-buffered saline at 37°C for 20 minutes and followed by one-step terminal-deoxynucleotidyl transferase mediated nick end labeling assay according to the manufactory's protocol from Elabscience (E-CK-A320).

The rehydrated slides were preheated in the antigen-repair solution (10 mM sodium citrate buffer, pH 6.0) at 95°C–100°C for 10 minutes and cooled at room temperature for 30 minutes and incubated with 5% bovine serum albumin (BSA) in Tris-HCl Buffer with Tween (TBST) for 30 minutes to block unspecific binding of the antibodies. Then, the diluted (1:200) primary antibody (CD206, PTM-6020, PTM BIO; CD11b, 21851-1-AP) 1% BSA in Phosphate Buffered Saline with Tween (PBST) were added onto the slides, respectively and incubated in a humidified dark chamber for overnight at 4°C. For immunohistochemistry, the tissue sections were treated with 3% H$_2$O$_2$ to block endogenous peroxidase before first antibody incubation and treated with horseradish peroxidase–labeled secondary antibodies and followed by DAB staining steps. For immunofluorescent staining, Coralite594-conjugated goat anti-rabbit IgG (H + L) or CoraLite488-conjugated goat anti-rabbit IgG (H + L) antibodies were used in 5% BSA at room temperature for 1 hour in the dark and followed by DAPI counterstaining. The

tissue morphologies and immunostaining signals were observed and photographed under Olympus BX63.

mIF Experiment

The 4-colored mIF performed using the mIF kit (AFIHC025, AiFang Biological, PRC) under its' guideline, and with diluted (1:200) primary antibody (CD206, 18704-1-AP, Proteintech; CD11b, 21851-1-AP, Proteintech; iNOS, 22226-1-AP, Proteintech; CCR2, 16153-1-AP, Proteintech; and CD86, 13395-1-AP, Proteintech) 1% BSA in PBST. Gamma settings were applied to each pixel in the image to eliminate background colors because of unavoidable stain residuals during the experiment.

Isolation and Culture of BMDMs

Mouse femur and tibia were sterilely isolated, and the bone marrow was rinsed out with 1640 complete medium. The bone marrow cells were collected by centrifugation at $500g$ at $4°C$ for 10 minutes to remove erythrocytes after mixing with red blood cell lysis buffer for 15 minutes and cultured at a final concentration of 2×10^6/mL with macrophage colony stimulating factor (Peprotech, 10 ng/mL) in 60 mm^2 cell culture dish at $37°C$ 5% CO_2 for 7 days to differentiate monocytes into BMDMs, which will be attached the culture dish.

qRT-PCR

Total RNAs were isolated using the TRIzol reagent. The first strand cDNA was reversely transcribed with oligo(dT) 12–18 primer and M-MLV reverse transcriptase (Promega). RT-PCR was performed with SYBR Green Master Mix kits (Roche Diagnosis) in ABI/ViiA7 Real-Time PCR System. The primers used in qRT-PCR were 5'- CTTCTTCGGTT CTGGAGGCT -3' and 5'- GGGATCTGAAGGCTGTCAAG -3' for Cdc42; 5'- CCAGTCGGGGACCAAGAACC -3' and 5'- CGTGG GTGGCAAAGAAAAGG -3' for SOCS3; 5'- TCTCCACGGAAA-CAGCATCT -3' and 5'- CTTACGGAAGCACCCATGAT -3' for CD86; 5'- CCACCACGCTCTTCTGTCTAC -3' and 5'- AGGGTC TGGGCCATAGAACT -3' for TNF-α; 5'- AGGTCAAAGGTTTG-GAAGCA -3' and 5'- TGAAGCAGCTATGGCAACTG -3' for IL1β; 5'- AACGATGATGCACTTGCAGA -3' and 5'- TGGTACTCCA-GAAGACCAGAGG-3' for IL6; 5'- TTGTGGTGAGCTGAAAGGTG -3' and 5'- GTGGATTGTCTTGTGGAGCA -3' for CD206; 5'- CCTGCTGTTCACAGTTGCC-3' and 5'-ATTGGGATCATCTTGCT GGT-3' for MCP1; 5'- ACCCAGAAGACTGTGGATGG -3' and 5'- ACACATTGGGGGTAGGAACA -3' for GAPDH.

Mouse Cytokine Antibody Array

The Mouse Cytokine Antibody Array kit was purchased from Abcam (ab133993). The array was conducted according to the manufacturer's protocol. In brief, the mouse sera or cell cultured media were added onto the membrane and incubated at $4°C$ for 12 hours, then the membranes were detected and photographed after biotinylated antibody incubation and chemiluminescent staining with horseradish peroxidase–streptavidin. The data were analyzed with ImageJ as the normalized intensity of the signal spots to positive control spots in the same membrane and displayed in heatmap.

Flow Cytometry Analysis

THP1 cells were pretreated with 50 ng/mL PMA (Sigma) for 48 hours, then stimulated with macrophage M2 polarization inducers IL4 and IL13 (both at 40 ng/mL, Peprotech) for 48 hours. THP1 or whole blood cells from mice were resuspended in Stain Buffer (BD, 554656) for 15 minutes. The THP1 cells were stained with CD11b-APC (BD, 550019), CD64-FITC (BD, 555527), CD86-FITC (BD, 557343), and CD206-FITC (BD, 551135). The whole blood cells were stained with Ly6C-PE/Cy7 (BioLegend, 128017), Ly6G-APC (BioLegend, 127613), CD11b-FITC (BioLegend, 101205), CD86-PE (BioLegend, 105106), and CD206-PerCP/Cy5.5 (BioLegend, 141716). The cells were detected on a Cyto-FLEX (Beckman Coulter). The results were analyzed by FlowJo v10.0.

Western Blot

The tissues or cells were lysed in RIPA buffer (50 mM Tris, 1% NP-40, 140 mM NaCl, and 0.1% sodium dodecyl sulfate, pH 7.6). The proteins were extracted and resolved by sodium dodecyl sulfate–polyacrylamide gel electrophoresis and transferred to a nitrocellulose membrane (GE Healthcare), which will be blocked with 5% BSA or skimmed milk in Tris-buffered saline containing 0.1% Tween 20 and probed with antibodies against iNOS (Proteintech, 22226-1-AP), ARG1 (Proteintech, 66129-1-AP), IL10 (proteintech,60269-1-Ig), IL6 (CST, 12912S), SOCS3 (Proteintech, 14025-1-AP), STAT Antibody Sampler Kit (CST, 9939T), Phospho-STAT Antibody Sampler (CST, 9914T: Phospho-STAT1 Tyr701 and Phospho-STAT3 Tyr705, Phospho-STAT6 Tyr641), respectively.

Statistical Analysis

The data were presented as the mean ± standard deviation and statistical analyses were processed by GraphPad Prism 9.0 statistical software with 2-way analysis of variance followed by Tukey's multiple comparisons test. $P < .05$ were considered as statistically significant.

References

1. Saidi RF, Kenari SK. Liver ischemia/reperfusion injury: an overview. J Invest Surg 2014;27:366–379.
2. Hirao H, Nakamura K, Kupiec-Weglinski JW. Liver ischaemia-reperfusion injury: a new understanding of the role of innate immunity. Nat Rev Gastroenterol Hepatol 2022;19:239–256.
3. Konishi T, Lentsch AB. Hepatic ischemia/reperfusion: mechanisms of tissue injury, repair, and regeneration. Gene Expr 2017;17:277–287.
4. Wen Y, Lambrecht J, Ju C, et al. Hepatic macrophages in liver homeostasis and diseases-diversity, plasticity and therapeutic opportunities. Cell Mol Immunol 2021; 18:45–56.

5. Liaskou E, Wilson DV, Oo YH. Innate immune cells in liver inflammation. Mediators Inflamm 2012;2012:949157.

6. Bilzer M, Roggel F, Gerbes AL. Role of Kupffer cells in host defense and liver disease. Liver Int 2006;26:1175–1186.

7. Krenkel O, Tacke F. Liver macrophages in tissue homeostasis and disease. Nat Rev Immunol 2017;17:306–321.

8. Stutchfield BM, Antoine DJ, Mackinnon AC, et al. CSF1 restores innate immunity after liver injury in mice and serum levels indicate outcomes of patients with acute liver failure. Gastroenterology 2015;149:1896–1909.

9. Nascimento M, Huang SC, Smith A, et al. Ly6Chi monocyte recruitment is responsible for Th2 associated host-protective macrophage accumulation in liver inflammation due to schistosomiasis. PLoS Pathog 2014;10:e1004282.

10. Zigmond E, Samia-Grinberg S, Pasmanik-Chor M, et al. Infiltrating monocyte-derived macrophages and resident Kupffer cells display different ontogeny and functions in acute liver injury. J Immunol 2014;193:344–353.

11. Scott CL, Zheng F, De Baetselier P, et al. Bone marrow-derived monocytes give rise to self-renewing and fully differentiated Kupffer cells. Nat Commun 2016;7:10321.

12. Dal-Secco D, Wang J, Zeng Z, et al. A dynamic spectrum of monocytes arising from the in situ reprogramming of CCR2+ monocytes at a site of sterile injury. J Exp Med 2015;212:447–456.

13. Yue S, Zhou H, Wang X, et al. Prolonged ischemia triggers necrotic depletion of tissue-resident macrophages to facilitate inflammatory immune activation in liver ischemia reperfusion injury. J Immunol 2017;198:3588–3595.

14. Wan P, Tan X, Xiang Y, et al. PI3K/AKT and CD40L signaling regulate platelet activation and endothelial cell damage in sepsis. Inflammation 2018;41:1815–1824.

15. Szondy Z, Sarang Z, Kiss B, et al. Anti-inflammatory mechanisms triggered by apoptotic cells during their clearance. Front Immunol 2017;8:909.

16. Huang Y, Xu Q, Zhang J, et al. Prussian blue scavenger ameliorates hepatic ischemia-reperfusion injury by inhibiting inflammation and reducing oxidative stress. Front Immunol 2022;13:891351.

17. Takai Y, Sasaki T, Matozaki T. Small GTP-binding proteins. Physiol Rev 2001;81:153–208.

18. Hall A. Rho GTPases and the actin cytoskeleton. Science 1998;279:509–514.

19. Comer FI, Parent CA. Phosphoinositides specify polarity during epithelial organ development. Cell 2007; 128:239–240.

20. Hall A. Rho GTPases and the control of cell behaviour. Biochem Soc Trans 2005;33:891–895.

21. Mogilner A, Allard J, Wollman R. Cell polarity: quantitative modeling as a tool in cell biology. Science 2012; 336:175–179.

22. Vojtek AB, Cooper JA. Rho family members: activators of MAP kinase cascades. Cell 1995;82:527–529.

23. Peng X, Lin Q, Liu Y, et al. Inactivation of Cdc42 in embryonic brain results in hydrocephalus with ependymal cell defects in mice. Protein Cell 2013;4:231–242.

24. Corry J, Mott HR, Owen D. Activation of STAT transcription factors by the Rho-family GTPases. Biochem Soc Trans 2020;48:2213–2227.

25. Nguyen P, Chakrabarti J, Li Y, et al. Rational targeting of Cdc42 overcomes drug resistance of multiple myeloma. Front Oncol 2019;9:958.

26. Mahendrarajah N, Borisova ME, Reichardt S, et al. HSP90 is necessary for the ACK1-dependent phosphorylation of STAT1 and STAT3. Cell Signal 2017; 39:9–17.

27. Nandy SB, Orozco A, Lopez-Valdez R, et al. Glucose insult elicits hyperactivation of cancer stem cells through miR-424-cdc42-prdm14 signalling axis. Br J Cancer 2017;117:1665–1675.

28. Lee JJ, Kim DH, Kim DG, et al. Toll-like receptor 4-linked Janus kinase 2 signaling contributes to internalization of Brucella abortus by macrophages. Infect Immun 2013; 81:2448–2458.

29. Fujimoto Y, Ochi H, Maekawa T, et al. A single nucleotide polymorphism in activated Cdc42 associated tyrosine kinase 1 influences the interferon therapy in hepatitis C patients. J Hepatol 2011;54:629–639.

30. Muzumdar MD, Tasic B, Miyamichi K, et al. A global double-fluorescent Cre reporter mouse. Genesis 2007; 45:593–605.

31. Arnold CE, Whyte CS, Gordon P, et al. A critical role for suppressor of cytokine signalling 3 in promoting M1 macrophage activation and function in vitro and in vivo. Immunology 2014;141:96–110.

32. Sica A, Mantovani A. Macrophage plasticity and polarization: in vivo veritas. J Clin Invest 2012;122:787–795.

33. Wilson HM. SOCS proteins in macrophage polarization and function. Front Immunol 2014;5:357.

34. Bode JG, Nimmesgern A, Schmitz J, et al. LPS and TNFalpha induce SOCS3 mRNA and inhibit IL-6-induced activation of STAT3 in macrophages. FEBS Lett 1999; 463:365–370.

35. Eltzschig HK, Eckle T. Ischemia and reperfusion: from mechanism to translation. Nat Med 2011;17:1391–1401.

36. Ye L, He S, Mao X, et al. Effect of hepatic macrophage polarization and apoptosis on liver ischemia and reperfusion injury during liver transplantation. Front Immunol 2020;11:1193.

37. Zhang M, Nakamura K, Kageyama S, et al. Myeloid HO-1 modulates macrophage polarization and protects against ischemia-reperfusion injury. JCI Insight 2018;3:e120596.

38. Wang H, Xi Z, Deng L, et al. Macrophage polarization and liver ischemia-reperfusion injury. Int J Med Sci 2021; 18:1104–1113.

39. Mills CD. Anatomy of a discovery: m1 and m2 macrophages. Front Immunol 2015;6:212.

40. Mantovani A, Biswas SK, Galdiero MR, et al. Macrophage plasticity and polarization in tissue repair and remodelling. J Pathol 2013;229:176–185.

41. Benoit M, Desnues B, Mege JL. Macrophage polarization in bacterial infections. J Immunol 2008;181:3733–3739.

42. O'Shea JJ, Schwartz DM, Villarino AV, et al. The JAK-STAT pathway: impact on human disease and therapeutic intervention. Annu Rev Med 2015;66:311–328.

43. Yasukawa H, Ohishi M, Mori H, et al. IL-6 induces an anti-inflammatory response in the absence of SOCS3 in macrophages. Nat Immunol 2003;4:551–556.

44. Stoiber D, Kovarik P, Cohney S, et al. Lipopolysaccharide induces in macrophages the synthesis of the suppressor of cytokine signaling 3 and suppresses signal transduction in response to the activating factor IFN-γ1. J Immunol 1999;163:2640–2647.

45. Wu F, Chen Y, Li Y, J, et al. RNA-interference-mediated Cdc42 silencing down-regulates phosphorylation of STAT3 and suppresses growth in human bladder-cancer cells. Biotechnol Appl Biochem 2008;49:121–128.

46. Lang R, Pauleau AL, Parganas E, et al. SOCS3 regulates the plasticity of gp130 signaling. Nat Immunol 2003; 4:546–550.

47. Clausen BE, Burkhardt C, Reith W, et al. Conditional gene targeting in macrophages and granulocytes using LysMcre mice. Transgenic Res 1999;8:265–277.

48. He XQ, Wang N, Zhao JJ, et al. Specific deletion of CDC42 in pancreatic β cells attenuates glucose-induced insulin expression and secretion in mice. Mol Cell Endocrinol 2020;518:111004.

49. Abe Y, Hines IN, Zibari G, et al. Mouse model of liver ischemia and reperfusion injury: method for studying reactive oxygen and nitrogen metabolites in vivo. Free Radic Biol Med 2009;46:1–7.

Correspondence
Address correspondence to: Hong-Bo Xin, PhD, The National Engineering Research Center for Bioengineering Drugs and Technology, Institute of Translational Medicine, Nanchang University, 1299 Xuefu Road, Honggutan District, Nanchang 330031, PR China. e-mail: xinhb@ncu.edu.cn; or Ke-Yu Deng, MD, The National Engineering Research Center for Bioengineering Drugs and Technology, Institute of Translational Medicine, Nanchang University, 1299 Xuefu Road, Honggutan District, Nanchang 330031, PR China. e-mail: dky@ncu.edu.cn.